CAUCHY – Jurnal Matematika Murni dan Aplikasi
Volume 11 (2) (2026), Pages 1–16
p-ISSN: 2086-0382; e-ISSN: 2477-3344

# Dynamic Analysis of Three-Species System with Fear Effect on Prey and Allee Effect on Top Predator

Dana Eky Novya and Dian Savitri*

*Department of Mathematics, Faculty of Mathematics and Natural Sciences, Universitas Negeri Surabaya, Indonesia*

**Abstract**

Fear-induced behavioral responses and low-density reproductive limitations can affect the stability and persistence of interacting populations. This study investigates a three-species system consisting of prey, middle predator, and top predator, incorporating a fear effect on prey growth and an Allee effect on top predator reproduction. The existence and local stability of biologically feasible equilibria are analyzed using the Jacobian matrix and Routh–Hurwitz criterion. Numerical continuation with MATCONT is employed to identify bifurcations associated with ecological and predation parameters, while numerical simulations are performed using the adaptive fourth–fifth order Runge–Kutta method. For the selected parameter set, two positive coexistence equilibria are obtained, with the first unstable and the second locally asymptotically stable. The continuation analysis reveals limit-point bifurcations for both the Allee-effect and fear-effect parameters. Further analysis shows that variation in the middle-predator predation rate $m_1$ produces two limit-point bifurcations, whereas variation in the top-predator predation rate $m_2$ generates one limit point and a subcritical Hopf bifurcation. The latter indicates the emergence of an unstable periodic orbit near $m_2 = 2.232969$. Numerical simulations confirm convergence toward the stable coexistence equilibrium with damped oscillatory transients. These results demonstrate that fear, Allee effects, and predation rates can alter the number and stability of coexistence equilibria and induce both equilibrium and oscillatory transitions in the three-species system.

**Keywords:** Allee effect; bifurcation analysis; fear effect; local stability; three-species system

Copyright © 2026 by Authors, Published by CAUCHY Group. This is an open access article under the CC BY-SA License (https://creativecommons.org/licenses/by-sa/4.0)

## 1. Introduction

Mathematical models of interacting populations provide a useful framework for studying population persistence, coexistence, and stability. In predator–prey systems, dynamics are governed not only by direct trophic interactions but also by behavioral responses and density-dependent demographic effects. One important behavioral mechanism is the fear effect, whereby predator presence alters prey behavior and reproduction, thereby modifying prey growth [1, 2]. Its inclusion can substantially affect equilibrium stability and temporal dynamics [3, 4].

Fear effects have also been incorporated into multi-species food-chain models. Cong et al. [2] studied a three-species food chain with predator-induced fear, while Pal et al. [5] examined fear effects in a three-species food chain with a generalist predator. These studies show that behavioral responses at one trophic level can influence the dynamics of the entire system. Delayed

*Corresponding author. E-mail: diansavitri@unesa.ac.id

Received: mm dd, yyyy Revised: mm dd, yyyy Accepted: mm dd, yyyy
DOI: https://doi.org/10.18860/cauchy.v11i2.xxxxx

fear effects have likewise been associated with stability switches and complex temporal behavior [1].

Another mechanism affecting population persistence is the Allee effect, which describes reduced population performance at low density. It may represent limitations in reproduction, mating, or other low-density processes and can alter the existence and stability of population equilibria [3, 6]. In food-chain models, such effects can influence the persistence and stability of interacting populations [7]. In particular, component Allee effects in predator reproduction provide a density-dependent mechanism linking predator persistence to its own population density [6].

The combined influence of fear and Allee effects has also been studied in several ecological models. Lai et al. [8] analyzed stability and bifurcation in a predator–prey model incorporating both effects, while Xie [4] examined their influence in a Holling type-II predator–prey system. Ratio-dependent and spatiotemporal formulations further showed that their interaction can modify equilibrium and bifurcation structures [9, 10]. For three-species food chains, Rana et al. [11] investigated the combined effects of fear and Allee mechanisms and their resulting complex dynamics.

More recently, Kumar et al. [12] considered a tri-trophic food chain in which fear affects the bottom prey and the Allee effect acts on the top predator. These studies provide a basis for combining behavioral and low-density effects in multi-trophic systems. However, the resulting equilibrium and stability structures depend on the specific functional forms and trophic interactions. This motivates a focused analysis of the equilibrium and bifurcation structure under the present three-species formulation.

In this study, we consider a three-species system consisting of prey ($x$), middle predator ($y$), and top predator ($z$). The prey experiences a fear effect that reduces its effective growth rate through the density-dependent factor $1/(1+\alpha y)$, where $\alpha$ measures the intensity of predator-induced fear. This formulation is consistent with previous fear-effect models [2, 11]. The top predator is subject to an Allee effect represented by $z/(\gamma+z)$, where $\gamma$ is the Allee-effect constant. Similar density-dependent formulations of predator reproduction have been considered in previous Allee-effect models [6, 11].

The objective of this study is to analyze the equilibrium structure and local stability of the proposed three-species system and to investigate bifurcations associated with its key ecological parameters. The positive coexistence equilibria are characterized analytically, while numerical continuation is employed to identify limit-point (LP) and Hopf bifurcations arising from variations in the fear, Allee, and predation parameters. Numerical simulations are subsequently used to illustrate the resulting population dynamics and complement the local stability analysis. Thus, the study focuses on how fear, Allee, and predation mechanisms shape coexistence, stability, and bifurcation behavior in the proposed three-species system.

## 2. Methods

The proposed system was analyzed using numerical integration and continuation to verify the analytical results and characterize its dynamics and bifurcations.

### 2.1. Numerical Integration and Stability Verification

System (1) was integrated in Python using `solve_ivp` with adaptive RK45, rtol $= 10^{-9}$, and atol $= 10^{-11}$. Time-series and phase-space simulations used $0 \le t \le 40$ and $0 \le t \le 150$, respectively, with 5000 equally spaced evaluation points. Positive initial conditions were used, with single and multiple conditions for the respective simulations.

### 2.2. Bifurcation Analysis and Numerical Continuation

One-parameter continuation was performed in MATCONT within MATLAB by varying $\gamma$, $\alpha$, $m_1$, and $m_2$ individually while fixing the remaining parameters. Predictor–corrector continuation with adaptive step sizes of 0.01, $10^{-5}$, and 0.1 (initial, minimum, and maximum), adaptation parameter 3, and 300 maximum points was used. Newton correction employed 3 Newton iterations, 10 correction iterations, and 10 test iterations, with variable/function tolerances $10^{-6}$, test tolerance $10^{-5}$, and Jacobian increment $10^{-5}$; TSearch order and Moore–Penrose options were enabled. LPs were identified by a simple zero eigenvalue and verified using the quadratic normal-form coefficient, while Hopf points were identified by a purely imaginary eigenvalue pair and characterized using the first Lyapunov coefficient.

## 3. Results and Discussion

### 3.1. Mathematical Model Formulation

We consider three interacting populations: prey ($x$), middle predator ($y$), and top predator ($z$). The prey grows logistically with intrinsic birth rate $b$, competition coefficient $a$, and mortality rate $d$, while the middle predator consumes the prey linearly with predation rate $m_1$ and efficiency $e_1$, and the top predator consumes the middle predator with rate $m_2$ and efficiency $e_2$, with natural mortalities $d_1$ and $d_2$, respectively. The middle predator induces a *fear effect* on the prey by reducing its birth rate through $1/(1+\alpha y)$, where $\alpha$ measures fear intensity. Meanwhile, the top predator experiences an *Allee effect* due to mating limitations at low densities, represented by $z/(\gamma+z)$, where $\gamma$ measures the Allee effect strength. Based on these assumptions, the system is formulated as the following non-linear autonomous ordinary differential equations:

$$\begin{aligned}
\frac{dx}{dt} &= \frac{bx}{1+\alpha y} - ax^2 - dx - m_1 xy, \\
\frac{dy}{dt} &= e_1 m_1 xy - d_1 y - m_2 yz, \\
\frac{dz}{dt} &= e_2 m_2 yz \left(\frac{z}{\gamma+z}\right) - d_2 z,
\end{aligned} \tag{1}$$

subject to the initial conditions $x(0) > 0$, $y(0) > 0$, and $z(0) > 0$. All parameters utilized in system (1) are assumed to be strictly positive, as summarized in Table 1.

**Table 1:** Ecological descriptions of the model parameters.

| Parameter | Biological Description |
|---|---|
| $b$ | Intrinsic birth rate of the prey |
| $a$ | Intraspecific competition rate of the prey |
| $d$ | Natural death rate of the prey |
| $\alpha$ | Intensity of the fear effect induced by the middle predator |
| $m_1$ | Predation rate of the middle predator on the prey |
| $e_1$ | Biomass conversion efficiency of the middle predator |
| $d_1$ | Natural death rate of the middle predator |
| $m_2$ | Predation rate of the top predator on the middle predator |
| $e_2$ | Biomass conversion efficiency of the top predator |
| $\gamma$ | Allee effect threshold constant (mating limitation) |
| $d_2$ | Natural death rate of the top predator |

### 3.2. Positivity and Boundedness

Let $x(0), y(0), z(0) > 0$. System (1) can be written as

$$\dot{x} = x\left(\frac{b}{1+\alpha y} - ax - d - m_1 y\right),\ \dot{y} \quad = y\left(e_1 m_1 x - d_1 - m_2 z\right),\ \dot{z} = z\left(e_2 m_2 y \frac{z}{\gamma + z} - d_2\right). \tag{2}$$

Since each equation contains its corresponding population variable as a factor, the coordinate planes are invariant. Hence, $\mathbb{R} * +^3$ is positively invariant and $x(t), y(t), z(t) \geq 0$ for all $t \geq 0$. To prove boundedness, define $N = x + y + z$. For $0 < e_1, e_2 \leq 1$ and $a, d, d_1, d_2 > 0$,

$$\dot{N} = \frac{bx}{1+\alpha y} - ax^2 - dx + (e_1 - 1)m_1 xy - d_1 y \qquad +(e_2 - 1)m_2 yz\frac{z}{\gamma + z} - d_2 z \leq \frac{b^2}{4a} - dx - d_1 y - d_2 z.$$

Let $\delta = \min d, d_1, d_2 > 0$. Since $dx + d_1 y + d_2 z \geq \delta N$,

$$\dot{N} \leq \frac{b^2}{4a} - \delta N, \tag{3}$$

and the comparison theorem yields

$$N(t) \leq N(0)e^{-\delta t} + \frac{b^2}{4a\delta}\left(1 - e^{-\delta t}\right). \tag{4}$$

Thus $\limsup * t \to \infty N(t) \leq b^2/(4a\delta)$, so all nonnegative solutions are bounded. Therefore, under the stated assumptions, system (1) is positively invariant and bounded in $\mathbb{R}^3_+$.

### 3.3. Existence and Stability Analysis of Equilibrium Points

The steady states of the formulated tri-trophic food chain system are evaluated to determine the operational states of the population dynamics. The fixed points are derived analytically by setting the temporal vector fields in system (1) to zero, which leads to the following algebraic system:

$$\begin{aligned} \frac{bx}{1+\alpha y} - ax^2 - dx - m_1 xy &= 0 \\ e_1 m_1 xy - d_1 y - m_2 yz &= 0 \\ e_2 m_2 yz\left(\frac{z}{\gamma + z}\right) - d_2 z &= 0 \end{aligned} \tag{5}$$

From the non-linear algebraic system (5), we systematically obtain all biologically feasible equilibrium points and state their boundaries of existence within the positive domain $\mathbb{R}^3_+$.

1. The trivial equilibrium point
$$E_0 = (0, 0, 0)$$
which always exists and corresponds to the total extinction of all populations.
2. The prey-only equilibrium point
$$E_1 = (x_1^*, 0, 0)$$
which represents the survival of the prey population in the absence of predators. Setting $y = 0$ and $z = 0$ in the first component of (5) yields
$$x_1^* = \frac{b - d}{a}.$$
The axial equilibrium $E_1$ physically exists in the positive domain provided that the survival criterion satisfies
$$b > d. \tag{6}$$

3. The planar top-predator-free equilibrium points

$$E_2 = (x_2^*, y_2^*, 0) \qquad \text{and} \qquad E_3 = (x_3^*, y_3^*, 0)$$

are obtained by setting $z = 0$ while maintaining $x > 0$ and $y \neq 0$. From the second equation of (5), we obtain

$$e_1 m_1 xy - d_1 y = 0.$$

For $y \neq 0$, it follows that

$$x_2^* = x_3^* = \frac{d_1}{e_1 m_1}.$$

Substituting this value into the first equation of (5) and multiplying by $(1 + \alpha y)$ yields the following quadratic equation for the middle predator density:

$$(m_1^2 \alpha e_1) y^2 + \left[ a\alpha d_1 + d\alpha e_1 m_1 + m_1^2 e_1 \right] y + [a d_1 + d e_1 m_1 - b e_1 m_1] = 0. \tag{7}$$

Let

$$A = m_1^2 \alpha e_1 > 0,$$

$$B = a\alpha d_1 + d\alpha e_1 m_1 + m_1^2 e_1 > 0,$$

and

$$C = a d_1 + d e_1 m_1 - b e_1 m_1.$$

Then (7) can be written in the standard form

$$Ay^2 + By + C = 0.$$

The two algebraic roots are given by

$$y_{2,3}^* = \frac{-B \pm \sqrt{\Delta}}{2A}, \qquad \Delta = B^2 - 4AC.$$

For a biologically feasible planar equilibrium, we require $y > 0$. Because $A > 0$ and $B > 0$, the existence of a positive root is determined by the sign of $C$. In particular, if $C < 0$, then

$$\frac{C}{A} < 0,$$

so that the two roots have opposite signs. Consequently, exactly one root is positive and the other is negative.
The condition $C < 0$ is equivalent to

$$b > d + \frac{a d_1}{e_1 m_1}. \tag{8}$$

Hence, under condition (8), the positive root defines the biologically feasible planar equilibrium

$$E_2 = (x_2^*, y_2^*, 0),$$

where

$$x_2^* = \frac{d_1}{e_1 m_1}, \qquad y_2^* > 0.$$

The second algebraic root satisfies

$$y_3^* < 0$$

and therefore gives the mathematical equilibrium

$$E_3 = (x_3^*, y_3^*, 0), \qquad x_3^* = \frac{d_1}{e_1 m_1},$$

which lies outside the biologically relevant region $\mathbb{R}^3_+$. Thus, $E_3$ is not a biologically feasible equilibrium and is excluded from the subsequent biological stability analysis.
Accordingly, the model possesses one biologically feasible planar equilibrium $E_2$ whenever condition (8) holds, while $E_3$ represents the nonphysical algebraic branch of the same planar equilibrium equation.

4. The positive interior coexistence equilibrium point

$$E_4 = (x^*, y^*, z^*)$$

where

$$x^* > 0, \qquad y^* > 0, \qquad z^* > 0.$$

From the third equation of (5), assuming $z^* \neq 0$, we obtain

$$e_2 m_2 y^* \left( \frac{z^*}{\gamma + z^*} \right) = d_2.$$

Solving for the top predator density gives

$$z^* = \frac{d_2 \gamma}{e_2 m_2 y^* - d_2}, \qquad y^* > \frac{d_2}{e_2 m_2}. \tag{9}$$

From the first equation of (5), since $x^* > 0$, we obtain

$$\frac{b}{1 + \alpha y^*} - a x^* - d - m_1 y^* = 0.$$

Hence,

$$x^* = \frac{1}{a} \left[ \frac{b}{1 + \alpha y^*} - d - m_1 y^* \right]. \tag{10}$$

Therefore, the positivity of $x^*$ requires

$$\frac{b}{1 + \alpha y^*} > d + m_1 y^*. \tag{11}$$

Finally, substituting (9) and (10) into the second equation of (5) yields a scalar equation for $y^*$:

$$\frac{e_1 m_1}{a} \left[ \frac{b}{1 + \alpha y^*} - d - m_1 y^* \right] - d_1 - \frac{m_2 d_2 \gamma}{e_2 m_2 y^* - d_2} = 0. \tag{12}$$

Hence, the positive interior equilibrium $E_4$ exists for every positive solution $y^*$ of (12) satisfying the feasibility conditions

$$y^* > \frac{d_2}{e_2 m_2} \tag{13}$$

and

$$\frac{b}{1 + \alpha y^*} > d + m_1 y^*. \tag{14}$$

The corresponding equilibrium components are then determined from

$$x^* = \frac{1}{a} \left[ \frac{b}{1 + \alpha y^*} - d - m_1 y^* \right]$$

and

$$z^* = \frac{d_2 \gamma}{e_2 m_2 y^* - d_2}.$$

Thus, the existence of the positive interior coexistence equilibrium is characterized by the existence of a positive solution $y^*$ satisfying (12) together with the feasibility conditions (13)–(14).

Now, we study the local stability of the dynamic system (1) around each equilibrium point. The Jacobian matrix of the system (1) is determined as:

$$J(x,y,z) = \begin{pmatrix} \dfrac{b}{1+\alpha y} - 2ax - d - m_1 y & -\dfrac{b\alpha x}{(1+\alpha y)^2} - m_1 x & 0 \\ e_1 m_1 y & e_1 m_1 x - d_1 - m_2 z & -m_2 y \\ 0 & \dfrac{e_2 m_2 z^2}{\gamma + z} & \dfrac{e_2 m_2 yz(2\gamma + z)}{(\gamma + z)^2} - d_2 \end{pmatrix}.$$

By evaluating the Jacobian matrix at each equilibrium point, the local stability properties of the equilibria are obtained as follows.

**Theorem 1.** *The total extinction equilibrium point $E_0 = (0,0,0)$ is locally asymptotically stable if $b < d$, and is unstable if $b > d$.*

*Proof.* The Jacobian matrix evaluated at $E_0$ is given by

$$J(E_0) = \begin{pmatrix} b-d & 0 & 0 \\ 0 & -d_1 & 0 \\ 0 & 0 & -d_2 \end{pmatrix}.$$

The characteristic equation is

$$(\lambda - (b-d))(\lambda + d_1)(\lambda + d_2) = 0.$$

Therefore, the eigenvalues are

$$\lambda_1 = b - d, \qquad \lambda_2 = -d_1, \qquad \lambda_3 = -d_2.$$

Since $d_1 > 0$ and $d_2 > 0$, the second and third eigenvalues are always negative. Thus, if $b < d$, all eigenvalues have negative real parts and $E_0$ is locally asymptotically stable. Conversely, if $b > d$, then $\lambda_1 > 0$, so $E_0$ is unstable.
At the threshold value $b = d$, one eigenvalue is zero and the equilibrium is non-hyperbolic. □

**Theorem 2.** *The axial predator-free fixed point $E_1$ of the system is locally asymptotically stable if*

$$b > d$$

*and*

$$d_1 > \frac{e_1 m_1 (b-d)}{a}.$$

*Proof.* The Jacobian matrix evaluated at equilibrium point $E_1$ is given by

$$J(E_1) = \begin{pmatrix} -(b-d) & -\dfrac{b\alpha(b-d)}{a} - \dfrac{m_1(b-d)}{a} & 0 \\ 0 & \dfrac{e_1 m_1 (b-d)}{a} - d_1 & 0 \\ 0 & 0 & -d_2 \end{pmatrix}.$$

The eigenvalues associated with the Jacobian matrix $J(E_1)$ are

$$\lambda_1 = -(b-d),$$

$$\lambda_2 = \frac{e_1 m_1 (b-d)}{a} - d_1,$$

and

$$\lambda_3 = -d_2.$$

Since $\lambda_1 < 0$ under $b > d$ and $\lambda_3 = -d_2 < 0$, the stability of $E_1$ depends on $\lambda_2 < 0$. Therefore,

$$d_1 > \frac{e_1 m_1 (b-d)}{a}$$

ensures that all eigenvalues have negative real parts. Hence, $E_1$ is locally asymptotically stable under the stated conditions. □

**Proposition 1.** *Under the existence condition (8), the two algebraic roots of the planar equilibrium equation have opposite signs. Hence, the equilibrium $E_2$ corresponds to the unique biologically feasible planar equilibrium, whereas $E_3$ lies outside the biological region $\mathbb{R}^3_+$.*

**Theorem 3.** *The biologically feasible planar top-predator-free equilibrium*

$$E_2 = (x_2^*, y_2^*, 0)$$

*is locally asymptotically stable whenever it exists.*

*Proof.* At the planar equilibrium $E_2 = (x_2^*, y_2^*, 0)$, the Jacobian matrix has the block-triangular form

$$J(E_2) = \begin{pmatrix} J_{11} & J_{12} & 0 \\ J_{21} & J_{22} & J_{23} \\ 0 & 0 & -d_2 \end{pmatrix},$$

where

$$\begin{aligned} J_{11} &= \frac{b}{1+\alpha y_2^*} - 2a x_2^* - d - m_1 y_2^*, \\ J_{12} &= -\frac{b\alpha x_2^*}{(1+\alpha y_2^*)^2} - m_1 x_2^*, \\ J_{21} &= e_1 m_1 y_2^*, \\ J_{22} &= e_1 m_1 x_2^* - d_1, \\ J_{23} &= -m_2 y_2^*. \end{aligned}$$

Since

$$x_2^* = \frac{d_1}{e_1 m_1},$$

we have

$$J_{22} = e_1 m_1 \left( \frac{d_1}{e_1 m_1} \right) - d_1 = 0.$$

Moreover, because $E_2$ satisfies the first equilibrium equation,

$$\frac{b}{1+\alpha y_2^*} - d - m_1 y_2^* = a x_2^*.$$

Therefore,

$$J_{11} = \frac{b}{1+\alpha y_2^*} - 2ax_2^* - d - m_1 y_2^* = -ax_2^* < 0.$$

The third eigenvalue is

$$\lambda_3 = -d_2 < 0.$$

The remaining two eigenvalues are determined by the upper-left $2 \times 2$ block, whose characteristic polynomial is

$$\lambda^2 + A_1\lambda + A_2 = 0,$$

where

$$A_1 = -J_{11} = ax_2^* > 0$$

and

$$A_2 = -J_{12}J_{21}.$$

Since

$$J_{12} = -\frac{b\alpha x_2^*}{(1+\alpha y_2^*)^2} - m_1 x_2^* < 0$$

and

$$J_{21} = e_1 m_1 y_2^* > 0,$$

we obtain

$$A_2 = -J_{12}J_{21} > 0.$$

Thus, by the Routh–Hurwitz criterion for a second-order polynomial, both eigenvalues associated with the upper-left $2 \times 2$ block have negative real parts. Together with

$$\lambda_3 = -d_2 < 0,$$

all eigenvalues of $J(E_2)$ have negative real parts.
Hence, the planar top-predator-free equilibrium $E_2$ is locally asymptotically stable whenever it exists. □

**Theorem 4.** *Let*

$$E_4 = (x^*, y^*, z^*), \qquad x^* > 0, \quad y^* > 0, \quad z^* > 0,$$

*be any biologically feasible positive coexistence equilibrium of system (1). Then $E_4$ is locally asymptotically stable if the coefficients of its characteristic polynomial*

$$\lambda^3 + a_1\lambda^2 + a_2\lambda + a_3 = 0$$

*satisfy the Routh–Hurwitz conditions*

$$a_1 > 0, \qquad a_2 > 0, \qquad a_3 > 0, \qquad a_1 a_2 > a_3.$$

*Proof.* The Jacobian matrix of system (1), evaluated at the positive coexistence equilibrium $E_4$, is given by

$$J(E_4) = \begin{pmatrix} J_{11} & J_{12} & 0 \\ J_{21} & J_{22} & J_{23} \\ 0 & J_{32} & J_{33} \end{pmatrix},$$

where

$$
\begin{aligned}
J_{11} &= \frac{b}{1+\alpha y^*} - 2ax^* - d - m_1 y^*, \\
J_{12} &= -\frac{b\alpha x^*}{(1+\alpha y^*)^2} - m_1 x^*, \\
J_{21} &= e_1 m_1 y^*, \\
J_{22} &= e_1 m_1 x^* - d_1 - m_2 z^*, \\
J_{23} &= -m_2 y^*, \\
J_{32} &= \frac{e_2 m_2 (z^*)^2}{\gamma + z^*}, \\
J_{33} &= \frac{e_2 m_2 y^* z^* (2\gamma + z^*)}{(\gamma + z^*)^2} - d_2.
\end{aligned}
$$

Since $E_4$ satisfies the first equilibrium equation,

$$\frac{b}{1+\alpha y^*} - ax^* - d - m_1 y^* = 0.$$

Therefore,

$$\frac{b}{1+\alpha y^*} - d - m_1 y^* = ax^*,$$

and hence

$$J_{11} = \frac{b}{1+\alpha y^*} - 2ax^* - d - m_1 y^* = -ax^* < 0.$$

The characteristic equation of $J(E_4)$ is obtained from

$$\det(\lambda I - J(E_4)) = 0,$$

and can be written as

$$\lambda^3 + a_1\lambda^2 + a_2\lambda + a_3 = 0,$$

where

$$
\begin{aligned}
a_1 &= -(J_{11} + J_{22} + J_{33}), \\
a_2 &= J_{11}J_{22} + J_{11}J_{33} + J_{22}J_{33} - J_{12}J_{21} - J_{23}J_{32}, \\
a_3 &= -J_{11}J_{22}J_{33} + J_{11}J_{23}J_{32} + J_{12}J_{21}J_{33}.
\end{aligned}
$$

For a third-order characteristic polynomial

$$\lambda^3 + a_1\lambda^2 + a_2\lambda + a_3 = 0,$$

the Routh–Hurwitz criterion states that all eigenvalues have negative real parts if and only if

$$a_1 > 0, \qquad a_2 > 0, \qquad a_3 > 0, \qquad a_1 a_2 > a_3.$$

Therefore, for any biologically feasible positive coexistence equilibrium $E_4$, if

$$a_1 > 0, \qquad a_2 > 0, \qquad a_3 > 0, \qquad a_1 a_2 > a_3,$$

then all eigenvalues of $J(E_4)$ have negative real parts. Consequently, $E_4$ is locally asymptotically stable. □

The stability conditions are applied separately to each biologically feasible positive coexistence equilibrium. Hence, when multiple positive coexistence equilibria exist under the same parameter set, their stability properties may differ. In particular, the existence of multiple coexistence equilibria does not imply that all of them are locally asymptotically stable.

A change in local stability occurs when the Routh–Hurwitz conditions are no longer satisfied. Therefore, the stability of each positive coexistence equilibrium is determined by evaluating the corresponding Routh–Hurwitz inequalities separately at that equilibrium.

### 3.4. Numerical Simulations

The numerical analysis was performed using the parameter set given in Table 2.

**Table 2:** Parameter values

| Parameter | Value | Biological meaning | Reference |
|---|---|---|---|
| $b$ | 3.80 | Intrinsic birth/growth rate of the prey | [13] |
| $a$ | 0.18 | Intraspecific competition coefficient of the prey | Assumed |
| $d$ | 0.15 | Natural mortality rate of the prey | [14] |
| $\alpha$ | 0.15 | Intensity of the fear effect | [15] |
| $m_1$ | 0.12 | Predation rate of the middle predator | Assumed |
| $e_1$ | 0.60 | Biomass conversion efficiency of the middle predator | [16] |
| $d_1$ | 0.12 | Natural mortality rate of the middle predator | [17] |
| $m_2$ | 0.10 | Predation rate of the top predator | [18] |
| $e_2$ | 0.50 | Biomass conversion efficiency of the top predator | [19] |
| $\gamma$ | 1.00 | Allee-effect constant | [20] |
| $d_2$ | 0.14 | Natural mortality rate of the top predator | Assumed |

The equilibrium system (5) admits two biologically feasible positive coexistence equilibria,

$$E_{4,1} = (2.30691511,\ 8.87403103,\ 0.46097888), \qquad E_{4,2} = (11.28881211,\ 3.20416027,\ 6.92794472).$$

Both equilibria satisfy $x^*, y^*, z^* > 0$. Their Jacobian eigenvalues are

$$E_{4,1}: \quad \lambda_{1,2} = -0.20330231 \pm 0.54061569i, \qquad \lambda_3 = 0.08718606,$$

and

$$E_{4,2}: \quad \lambda_1 = -1.32247438, \qquad \lambda_{2,3} = -0.34592637 \pm 0.12707197i.$$

Hence, $E_{4,1}$ is unstable, whereas $E_{4,2}$ is locally asymptotically stable. These results are consistent with the Routh–Hurwitz analysis.

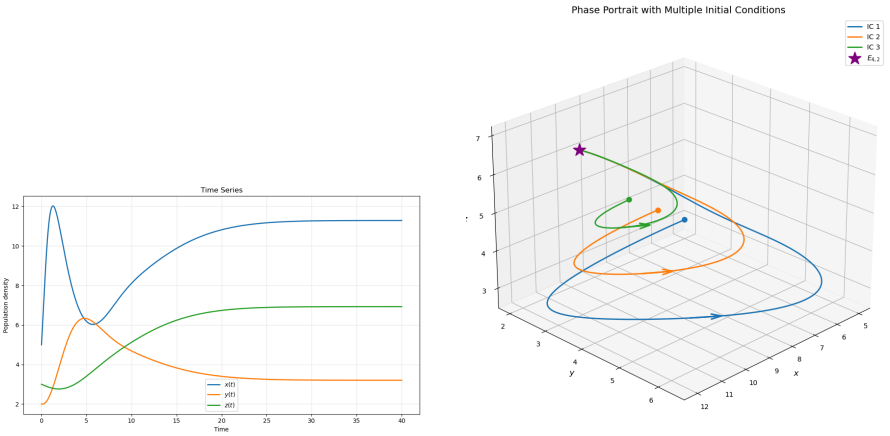
The numerical trajectories were obtained using RK45 with rtol $= 10^{-9}$ and atol $= 10^{-11}$. Figure 1(a) shows the time-series dynamics from

$$(x(0), y(0), z(0)) = (5, 2, 3), \qquad 0 \le t \le 40.$$

The populations exhibit transient oscillations before approaching $E_{4,2}$. Figure 1(b) presents the three-dimensional phase portrait for

$$(5, 2, 3), \qquad (7, 2.5, 4), \qquad (9, 3, 5),$$

over $0 \le t \le 150$. Although the trajectories have different transient paths, they approach the same positive coexistence equilibrium $E_{4,2}$, consistent with its locally asymptotically stable character.




**(a)** Time-series dynamics of $(x)$, $(y)$, and $(z)$.

**(b)** Three-dimensional phase portrait for multiple initial conditions.

**Fig. 1:** Numerical dynamics of the tri-trophic food-chain system showing convergence toward the stable coexistence equilibrium $E_{4,2}$.

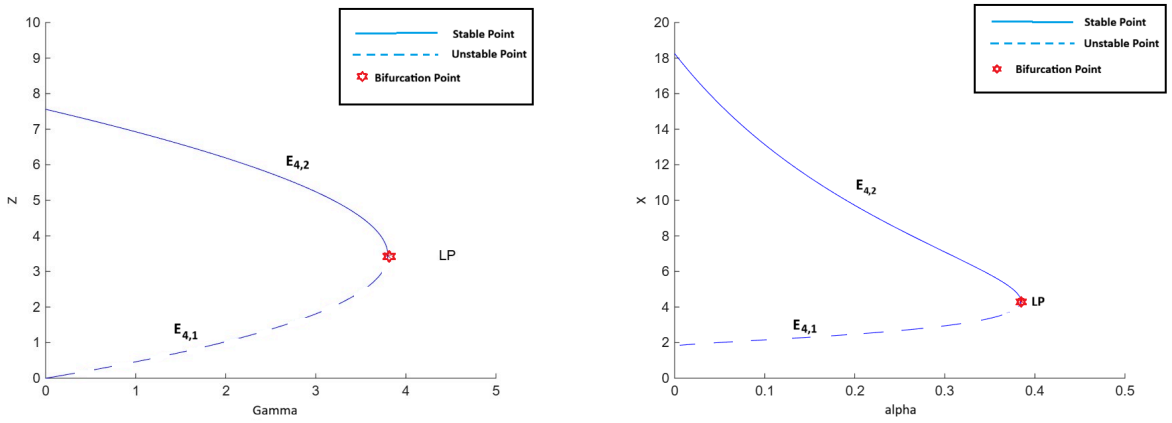
## 3.5. Bifurcation Analysis

The bifurcation behavior of system (1) was investigated using MATCONT via one-parameter equilibrium continuation, with the Allee-effect parameter $\gamma$ and fear-effect parameter $\alpha$ varied separately while other parameters were fixed. The initial, minimum, and maximum step sizes were 0.01, $10^{-5}$, and 0.1, respectively, with adaptation parameter 3 and 300 maximum continuation points; closed-branch checking was performed every 50 points. The Newton correction used at most 3 Newton iterations, 10 correction iterations, and 10 test iterations, with variable, function, and test tolerances of $10^{-6}$, $10^{-6}$, and $10^{-5}$, respectively. The Jacobian increment was $10^{-5}$, with TSearch order and Moore–Penrose options enabled. Critical points were detected from Jacobian singularities, with a limit point (LP) identified as a fold of the equilibrium branch associated with a zero eigenvalue.

### *3.5.1. Limit Point Bifurcations Induced by Allee and Fear Effects*

For the Allee effect, $\gamma$ was varied as the single free parameter and the top-predator density $z^*$ was used as the state variable. A limit point (LP) was detected at $\gamma_{\mathrm{LP}} = 3.799530$, with the corresponding equilibrium $(x, y, z, \gamma) = (6.469650, 5.876411, 3.458148, 3.799530)$. The quadratic normal-form coefficient at the LP is $a = -9.920180 \times 10^{-3} \neq 0$, confirming the nondegeneracy condition for a generic fold (saddle-node) bifurcation. The positive coexistence equilibrium $E_4$ has two branches, with the lower branch $E_{4,1}$ being unstable and the upper branch $E_{4,2}$ being stable. At $\gamma = \gamma_{\mathrm{LP}}$, these two positive equilibrium branches coalesce at the limit point. The Jacobian has a simple zero eigenvalue at this point, indicating that two nearby coexistence equilibria coalesce at $\gamma_{\mathrm{LP}}$ and disappear on the other side of the fold.

Similarly, the fear effect was examined by varying $\alpha$ and tracking the prey density $x^*$. The continuation detected a limit point (LP) at $\alpha_{\mathrm{LP}} = 0.384437$, with $E_{\mathrm{LP}} = (4.337647, 4.255978, 1.923106)$. The corresponding quadratic normal-form coefficient is $a = -1.179004 \times 10^{-2} \neq 0$, confirming a generic fold bifurcation. The positive coexistence equilibrium $E_4$ exhibits two branches, denoted by $E_{4,1}$ and $E_{4,2}$, where $E_{4,1}$ is unstable and $E_{4,2}$ is stable. At $\alpha = \alpha_{\mathrm{LP}}$, these two positive equilibrium branches coalesce at the turning point. The stability of both continued branches was assessed from the Jacobian eigenvalues: an equilibrium is locally asymptotically stable when all eigenvalues have negative real parts and unstable when at least one has a positive real part. The resulting bifurcation diagrams therefore demonstrate that both the Allee-effect parameter $\gamma$ and fear-effect parameter $\alpha$ can alter the existence and stability of positive coexistence equilibria.




**(a)** Allee effect: $\gamma$–$z^*$ diagram. **(b)** Fear effect: $\alpha$–$x^*$ diagram.

**Fig. 2:** Limit point bifurcations induced by (a) the Allee effect and (b) the fear effect.

### *3.5.2. Limit Point Bifurcations Induced by Middle-Predator Predation*

The effect of $m_1$, representing the predation rate of the middle predator on the prey $x$, was investigated by continuation of the positive coexistence equilibrium branch. Two limit points (LP1 and LP2) were detected at $(x, y, z, m_1) = (8.808777, 6.175214, 0.829577, 0.038401)$ and $(2.228124, 3.184487, 7.282434, 0.634497)$, respectively. The corresponding quadratic normal-form coefficients are $a = -2.219361 \times 10^{-2} \neq 0$ and $a = -2.132606 \times 10^{-3} \neq 0$. Thus, both LP1 and LP2 satisfy the nondegeneracy condition for generic fold (saddle-node) bifurcations. The continuation diagram shows a stable and an unstable positive coexistence branch between the two limit points, indicating that the fold structure is associated with the coexistence equilibrium $E_4$. Thus, variation in the predation rate of the middle predator on the prey $x$ produces two turning points along the coexistence-equilibrium branch, where pairs of nearby equilibria coalesce. These results indicate that changes in $m_1$ can alter the number of positive coexistence equilibria through multiple saddle-node bifurcations.

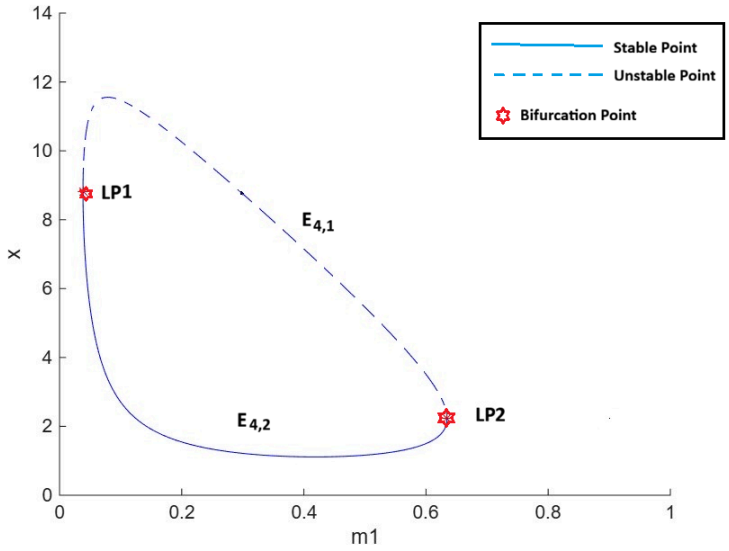



**Fig. 3:** Limit point bifurcations induced by the predation rate $m_1$ of the middle predator on the prey $x$.

### *3.5.3. Bifurcations Induced by Top-Predator Predation*

The effect of $m_2$, representing the predation rate of the top predator on the middle predator $y$, was investigated by continuing the positive coexistence equilibrium branch. The analysis revealed

one Hopf bifurcation and one limit point along the $E_4$ equilibrium branch. The Hopf point was detected at $(x, y, z, m_2) = (18.991899, 0.349857, 0.558636, 2.232969)$, with the first Lyapunov coefficient $l_1 = 3.836475 \times 10^{-4} > 0$, indicating a subcritical Hopf bifurcation and the emergence of an unstable periodic orbit near the critical value $m_2 = 2.232969$.

A limit point was also detected at $(x, y, z, m_2) = (3.964817, 7.600139, 3.491324, 0.047394)$, with quadratic normal-form coefficient $a = -6.483749 \times 10^{-3} \neq 0$. Hence, the nondegeneracy condition is satisfied, confirming a generic fold (saddle-node) bifurcation. The continuation diagram shows that the positive coexistence equilibrium is stable between the limit point and the Hopf point, while it becomes unstable after the Hopf bifurcation. Thus, variation in $m_2$ induces both a saddle-node bifurcation, which changes the number of positive coexistence equilibria, and a subcritical Hopf bifurcation, which changes their stability and generates an unstable periodic orbit.

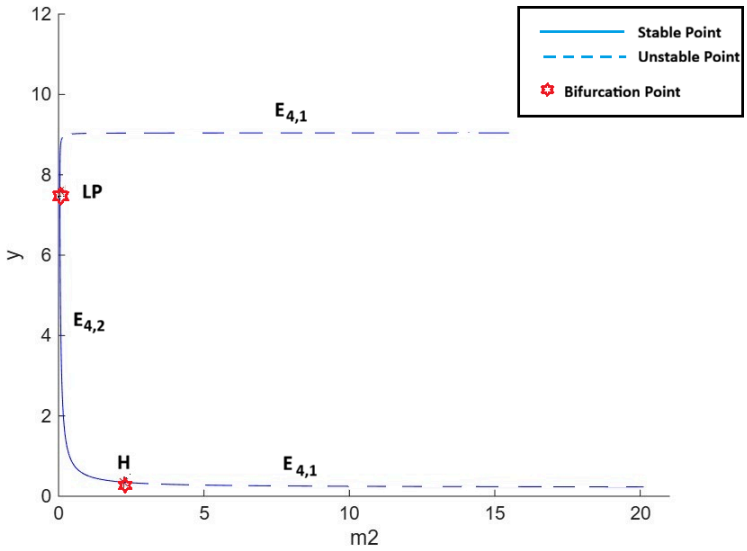



**Fig. 4:** Bifurcation diagram with respect to the predation rate $m_2$ of the top predator on the middle predator $y$.

## 4. Conclusion

This study investigated a three-species system incorporating predator-induced fear in the prey and an Allee effect in the top predator, focusing on coexistence equilibria, local stability, and bifurcations. Multiple biologically feasible coexistence equilibria were shown to occur under the same parameter regime with different stability properties, while numerical simulations confirmed convergence to the locally asymptotically stable coexistence state.

MATCONT continuation showed that the Allee-effect parameter $\gamma$ and fear-effect parameter $\alpha$ can induce limit point bifurcations and alter the equilibrium structure. Predation rates also strongly affect the dynamics: variation in $m_1$ produced two limit point bifurcations, indicating multiple saddle-node transitions and changes in the number of positive coexistence equilibria, whereas variation in $m_2$ produced a limit point and a subcritical Hopf bifurcation, indicating both equilibrium transitions and oscillatory instability. Thus, trophic interaction rates are important in determining persistence and stability.

The equilibrium analysis, Routh–Hurwitz criteria, numerical simulations, and MATCONT continuation provide a systematic framework for identifying equilibrium and oscillatory transitions. Future work may extend this analysis to two-parameter bifurcations and broader parameter regimes to explore the interactions among fear, Allee effects, and predation rates.

## CRediT Authorship Contribution Statement

**Dana Eky Novya:** Conceptualization, Methodology, Software, Formal Analysis, Investigation, Writing–Original Draft, Visualization. **Dian Savitri:** Conceptualization, Methodology, Validation, Writing–Review & Editing, Visualization, Supervision.

## Declaration of Generative AI and AI-assisted technologies

During the development of this study, the authors used ChatGPT (GPT-5.6 Luna) to assist with manuscript organization, initial drafting, and language refinement. The authors reviewed and revised the generated content and take full responsibility for the final manuscript.

## Declaration of Competing Interest

The authors declare no competing interests.

## Ethics Approval and Consent to Participate

Ethics approval was not required for this study.

## Funding and Acknowledgments

The authors sincerely thank their supervisor for valuable guidance and support throughout the research, and their colleagues for their assistance and contributions to this manuscript.

## Data and Code Availability

The Python codes for numerical simulations and the MATCONT files for numerical continuation and bifurcation analysis can be accessed through the following GDrive repository: [1].

## References

[1] Pijush Panday, Sudip Samanta, Nikhil Pal, and Joydev Chattopadhyay. "Delay induced multiple stability switch and chaos in a predator–prey model with fear effect". In: *Mathematics and Computers in Simulation* 172 (2020), pp. 134–158. DOI: 10.1016/j.matcom.2019.12.015.

[2] Pingping Cong, Meng Fan, and Xingfu Zou. "Dynamics of a three-species food chain model with fear effect". In: *Communications in Nonlinear Science and Numerical Simulation* 99 (2021), p. 105809. DOI: 10.1016/j.cnsns.2021.105809.

[3] Ying Huang, Zhenliang Zhu, and Zhong Li. "Modeling the Allee effect and fear effect in predator–prey system incorporating a prey refuge". In: *Advances in Difference Equations* 2020.1 (2020), p. 321. DOI: 10.1186/s13662-020-02727-5.

[4] Binfeng Xie. "Impact of the fear and Allee effect on a Holling type II prey–predator model". In: *Advances in Difference Equations* 2021.1 (2021), p. 464. DOI: 10.1186/s13662-021-03592-6.

[5] Soumitra Pal, Pankaj Kumar Tiwari, Arvind Kumar Misra, and Hao Wang. "Fear effect in a three-species food chain model with generalist predator". In: *Mathematical Biosciences and Engineering* 21.1 (2024), pp. 1–33. DOI: 10.3934/mbe.2024001.

[6] Udai Kumar and Partha Sarathi Mandal. "Role of Allee effect on prey–predator model with component Allee effect for predator reproduction". In: *Mathematics and Computers in Simulation* 193 (2022), pp. 623–665. DOI: 10.1016/j.matcom.2021.10.027.

[1] https://drive.google.com/drive/folders/1VPmxrpQ_h8UxK72_IyQuDCzew4xCJIJf?usp=sharing]

[7] S. Vinoth, R. Sivasamy, K. Sathiyanathan, Grienggrai Rajchakit, P. Hammachukiattikul, R. Vadivel, and Nallappan Gunasekaran. "Dynamical analysis of a delayed food chain model with additive Allee effect". In: *Advances in Difference Equations* 2021.1 (2021), p. 54. DOI: 10.1186/s13662-021-03216-z.

[8] Liyun Lai, Zhenliang Zhu, and Fengde Chen. "Stability and Bifurcation in a Predator–Prey Model with the Additive Allee Effect and the Fear Effect". In: *Mathematics* 8.8 (2020), p. 1280. DOI: 10.3390/math8081280.

[9] Yajing Li, Mengxin He, and Zhong Li. "Dynamics of a ratio-dependent Leslie–Gower predator–prey model with Allee effect and fear effect". In: *Mathematics and Computers in Simulation* 201 (2022), pp. 417–439. DOI: 10.1016/j.matcom.2022.05.017.

[10] Changcheng Ke, Ming Yi, and Yanfeng Guo. "Qualitative Analysis of a Spatiotemporal Prey–Predator Model with Additive Allee Effect and Fear Effect". In: *Complexity* 2022 (2022), p. 5715922. DOI: 10.1155/2022/5715922.

[11] Sourav Rana, Sabyasachi Bhattacharya, and Sudip Samanta. "Complex Dynamics of a Three-Species Food Chain Model with Fear and Allee Effect". In: *International Journal of Bifurcation and Chaos* 32.6 (2022), p. 2250084. DOI: 10.1142/S0218127422500845.

[12] Vinay Kumar, Suneel Kumar Bairwa, and Tanvi. "Influence of fear and Allee effects on stability and species survival in a tri-trophic food chain". In: *Communications in Nonlinear Science and Numerical Simulation* 152 (2026), p. 109115. DOI: 10.1016/j.cnsns.2025.109115.

[13] S. Mukherjee. "Dynamics of a Discrete-Time Ecogenetic Predator-Prey Model". In: *Computational and Mathematical Biophysics* 5.2 (2022). DOI: 10.5614/cbms.2022.5.2.5.

[14] Roy Subana. "Bistability in a Predator-Prey Model Characterized by the Crowley-Martin Functional Response". In: *Mathematics and Computers in Simulation* (2024). DOI: 10.1016/j.matcom.2024.09.001.

[15] X. Meng, L. Chen, and F. Chen. "Dynamics of a Predator-Prey System with Asymmetric Dispersal and Fear Effect". In: *Symmetry* 17.3 (2025), p. 329. DOI: 10.3390/sym17030329.

[16] Jake M. Ferguson, John B. Hopkins, and Briana H. Witteveen. "Integrating Abundance and Diet Data to Improve Inferences of Food Web Dynamics". In: *Methods in Ecology and Evolution* 9.6 (2018). DOI: 10.1111/2041-210X.13001.

[17] Anna Kuparinen and Jeffrey A. Hutchings. "Increased Natural Mortality at Low Abundance Can Generate an Allee Effect in a Marine Fish". In: *Royal Society Open Science* 1.2 (2014), p. 140075. DOI: 10.1098/rsos.140075.

[18] Vinay Kumar, Suneel Kumar Bairwa, and Tanvi. "Influence of Fear and Allee Effects on Stability and Species Survival in a Tri-Trophic Food Chain". In: *Communications in Nonlinear Science and Numerical Simulation* 152 (2026), p. 109115. DOI: 10.1016/j.cnsns.2025.109115.

[19] Karin A. Nilsson, Kevin S. McCann, and Amanda L. Caskenette. "Interaction Strength and Stability in Stage-Structured Food Web Modules". In: *Oikos* 127.10 (2018), pp. 1494–1505. DOI: 10.1111/oik.05029.

[20] Shuangte Wang and Hengguo Yu. "Complexity Analysis of a Modified Predator-Prey System with Beddington–DeAngelis Functional Response and Allee-Like Effect on Predator". In: *Discrete Dynamics in Nature and Society* (2021), p. 5618190. DOI: 10.1155/2021/5618190.